Molecular Medicine

Supplemental Data

Reduction of Cellular Expression Levels Is a Common Feature of Functionally Affected Pendrin (SLC26A4) Protein Variants

Vanessa C S de Moraes,[1] Emanuele Bernardinelli,[2]* Nathalia Zocal,[1] Jhonathan A Fernandez,[1] Charity Nofziger,[2] Arthur M Castilho,[3] Edi L Sartorato,[1] Markus Paulmichl,[2] and Silvia Dossena[2]*

Online address: http://www.molmed.org

Feinstein Institute for Medical Research
Northwell Health™

SUPPLEMENTARY MATERIALS AND METHODS

Cell Culture and Transient Transfection

HEK 293 Phoenix and HeLa cells were cultured in Minimum Essential Eagle Medium (MEM, Sigma-Aldrich, Austria) supplemented with 10% fetal bovine serum (FBS, Lonza), 2 mM L-glutamine, 100 U/ml penicillin, 100 μg/ml streptomycin and 1 mM pyruvic acid (sodium salt). The cells were maintained at 37 °C, 5% CO_2, 95% air and 100% humidity. Subcultures were routinely established every second to third day by seeding the cells into 100 mm diameter Petri dishes following trypsin/ethylenediaminetetraacetic acid (EDTA) treatment.

For functional tests (fluorometric method), HEK 293 Phoenix cells were seeded into black 96-multiwells, grown overnight and transfected with a total amount of 0.2 μg/well of plasmid DNA by the calcium phosphate co-precipitation method. Functional tests were performed 48 h post-transfection.

For western blots, HEK 293 Phoenix cells were seeded into 6-well plates, grown overnight and transfected with a total amount of 2 μg/well of plasmid DNA by the calcium phosphate co-precipitation method. Transfection medium was replaced with fresh medium 8 h post-transfection and cells were collected 72 h post-transfection.

For co-localization and determination of pendrin expression levels and transfection efficiency by imaging, HeLa cells were seeded into 6-well plates, grown overnight and transfected with 1.5 μg of plasmid DNA and 3 μl of Metafectene Pro (Biontex). Transfection medium was replaced with fresh medium 8 h post-transfection. Cells were transferred on round (3 cm diameter) glass slides 48 h post-transfection and imaged 72 h post-transfection.

Functional Test

The functional test was performed as already described, with adaptations allowing for the use of a multiplate reader (1-3). Shortly, cells were co-transfected with 0.1 μg of a plasmid encoding for EYFP p.H148Q;I152L (an EYFP variant with substantially improved sensitivity for iodide (4)) and 0.1 μg of pTARGET plasmid bearing the cDNA of wild type or mutated pendrin. Control cells were co-transfected with EYFP p.H148Q;I152L and the empty pTARGET vectors. Cells were washed from the culture medium and bathed in 70 μl of high chloride solution (in mM: KCl 2, NaCl 135, $CaCl_2$ 1, $MgCl_2$ 1, D-glucose 10, 4-(2-hydroxyethyl)-1-piperazineethane sulfonic acid (HEPES) 20, 308 mOsm/KgH_2O with mannitol, pH 7.4). After measuring the fluorescence intensity (1 measurement/second for 3 s), 140 μl of high iodide solution (in mM: KCl 2, NaI 135, $CaCl_2$ 1, $MgCl_2$ 1, D-glucose 10, HEPES 20, 308 mOsm/KgH_2O with mannitol, pH 7.4) were injected into each well. Then, the fluorescence intensity was measured again (1 measurement/second for 16 s). Since pendrin can act as a chloride/iodide exchanger (5-7), the presence of iodide in the extracellular medium induces an iodide flux into the cytoplasm of pendrin-expressing cells. Iodide is a much better quencher of EYFP p.H148Q;I152L fluorescence than chloride, therefore, an increase in intracellular iodide leads to a decrease of EYFP p.H148Q;I152L fluorescence (4) that reflects pendrin transport efficiency.

Fluorescence intensity was detected with the *VICTOR™ X3* Multilabel Plate Reader (Perkin Elmer) equipped with a liquid dispenser and the following filters: excitation: F485 (excitation center wavelength (CWL): 485 nm, bandwidth: 14 nm), emission: F535 (emission CWL: 535 nm, bandwidth: 25 nm). The background fluorescence measured in cells transfected with 0.2 μg of the pTARGET vector only was subtracted from all other fluorescence measurements of a same 96-well plate. Transport activity of cells expressing pendrin variants was statistically compared to the transport activity of cells expressing wild type pendrin or control cells seeded on the same 96-well plate. The technical necessity to have wild type and variant pendrin-expressing cells, control cells and cells for background determination on the same plate limited the number of pendrin variants that could be characterized simultaneously.

Co-localization Experiments

To stain the PM, living cells were washed three times with ice-cold Hank's

balanced salt solution (HBSS, Sigma-Aldrich), incubated on ice for 5 min with 1.25 μg/ml CellMask™ Deep Red plasma membrane stain (C10046, Invitrogen Molecular Probes) in HBSS, washed again three times with ice-cold HBSS and imaged immediately in HBSS. To stain the ER, living cells were washed three times with room temperature HBSS, incubated for 20 min at 37 °C and 5% CO_2 with 1 μM ER-Tracker™ Red (glibenclamide BODIPY®TR, E34250, Invitrogen Molecular Probes) in Krebs-Henseleit buffer (Sigma-Aldrich), washed again three times and immediately imaged in HBSS at room temperature.

For co-localization with the PM, EYFP was excited with the 514 nm line of the Argon laser and emission was detected in the 525-600 nm range; the CellMask™ Deep Red stain was excited at 633 nm (HeNe laser) and emission was detected in the 655-750 nm range. For co-localization with the ER, EYFP was excited with the 514 nm line of the Argon laser and emission was detected in the 525-555 nm range; ER-Tracker™ Red was excited at 561 nm (diode-pumped solid-state (DPSS) laser) and emission was detected in the 571-650 nm range.

In Figure 2, the presence of white (PM) or yellow (ER) pixels in the overlay images and the distribution of pixels along the diagonal in the scatter plots are indicative of co-localization between the two signals. Similarly, the absence of white (PM) or yellow (ER) pixels in the merge image and the distribution of pixels along the x and y axes in the scatter plots are indicative of an absence of co-localization between the two signals.

Co-localization with PM or ER markers was quantified and expressed as the Pearson's correlation coefficient (8), that may range from -1 to +1 indicating complete spatial exclusion (-1) or co-localization (+1) of a fluorescent signal with the marker of interest. Localization of EYFP, a water soluble protein with apparent homogeneous distribution within the intracellular compartments including the ER, was taken as an indicator of an absence of preferential localization with the PM.

Determination of Wild-type and Mutant Pendrin Expression Levels in Total Cell Membranes Lysates by Western Blot

Samples for SDS-PAGE were prepared by adding a denaturing loading dye containing 100 mM dithiothreitol and 8% SDS to the pellet corresponding to the total cellular membranes fraction. Samples were boiled for 5 min before loading on a 7.5% polyacrylamide gel. Separated proteins were transferred on polyvinylidene difluoride membranes (Immunoblot PVDF Membranes, BIO-RAD, Germany) by applying a constant voltage (75 V) for 2 h at 4 °C. The membranes were blocked for 1 h at room temperature in 5% nonfat dry milk in Tris-buffered saline and 0.1% Tween 20 (TBST), cut horizontally in two parts and incubated overnight at 4 °C with the primary antibody (rabbit anti-pendrin, 1:10,000, kindly provided by Prof. D Eladari, or rabbit anti-calreticulin, ab4, Abcam, 1:1,000) in 3% nonfat dry milk in phosphate buffered saline (PBS). Membranes were successively washed three times in TBST, incubated for 1 h at room temperature with infrared dye-conjugated secondary antibodies (goat anti-rabbit IRDye 800CW conjugated, LI-COR, USA, 1:20,000 dilution in 3% nonfat dry milk in PBS) and washed three times in TBST.

Determination of Wild-type and Mutant Pendrin Total Expression Levels by Imaging

EYFP was excited with the 514 nm line of the Argon laser and emission was detected between 525 and 597 nm; DAPI was excited with a diode laser (405 nm) and emission was detected between 430 and 470 nm. Laser power and photomultipliers gain were kept rigorously constant for acquisition of all images.

Determination of Wild-type and Mutant Pendrin Expression Levels in the Plasma Membrane Region

EYFP was excited with the 514 nm line of the Argon laser and emission was detected between 525 and 580 nm. ECFP was excited with a diode laser (405 nm) and emission was detected between 450 and 490 nm. CellMask™ Deep Red stain was excited at 633 nm (HeNe laser) and emission was detected in the 643-750 nm range. Laser power and photomultipliers gain were kept rigorously constant for acquisition of all images.

Verification of Transfection Efficiency by Imaging

As differences in the activity and expression levels of the pendrin variants could potentially arise from differences in the transfection efficiency of the corresponding plasmid constructs, the latter was further verified by imaging for wild type pendrin and two representative pendrin variants with and without functional impairment, *i.e.* T193I and R776C, respectively. For this, the ORF of PDS-EYFP was subcloned into the pIRES2-DsRed-Express vector (Clontech), coding for the fluorescent protein DsRed. The mRNA generated following transcription of this construct (pIRES2-DsRed-Express PDS-EYFP) contains the PDS-EYFP and the DsRed coding sequences separated by an internal ribosomal entry site (IRES) (9). Following transfection of this construct, PDS-EYFP expressing cells simultaneously also express DsRed as an independent protein.

Following transfection, PDS-EYFP and DsRed are translated as individual proteins from the same bicistronic mRNA. Transfected and pendrin-expressing living HeLa cells were identified based on the expression of DsRed and EYFP, respectively, and sequentially imaged following excitation of EYFP at 514 nm (emission: 524-555 nm) and DsRed at 561 nm (emission: 571-660 nm). The number of transfected (DsRed positive) and pendrin expressing (EYFP positive) cells was then determined. All of the transfected (DsRed-expressing) cells also expressed wild type pendrin or pendrin R776C (Supplementary Table S3). In contrast, only a minority of the transfected (DsRed-expressing) cells expressed pendrin T193I (Supplementary Table S3), therefore evidencing that possible differences in transport activity and expression levels of pendrin variants do not arise from a reduction in the transfection efficiency of the corresponding plasmid construct.

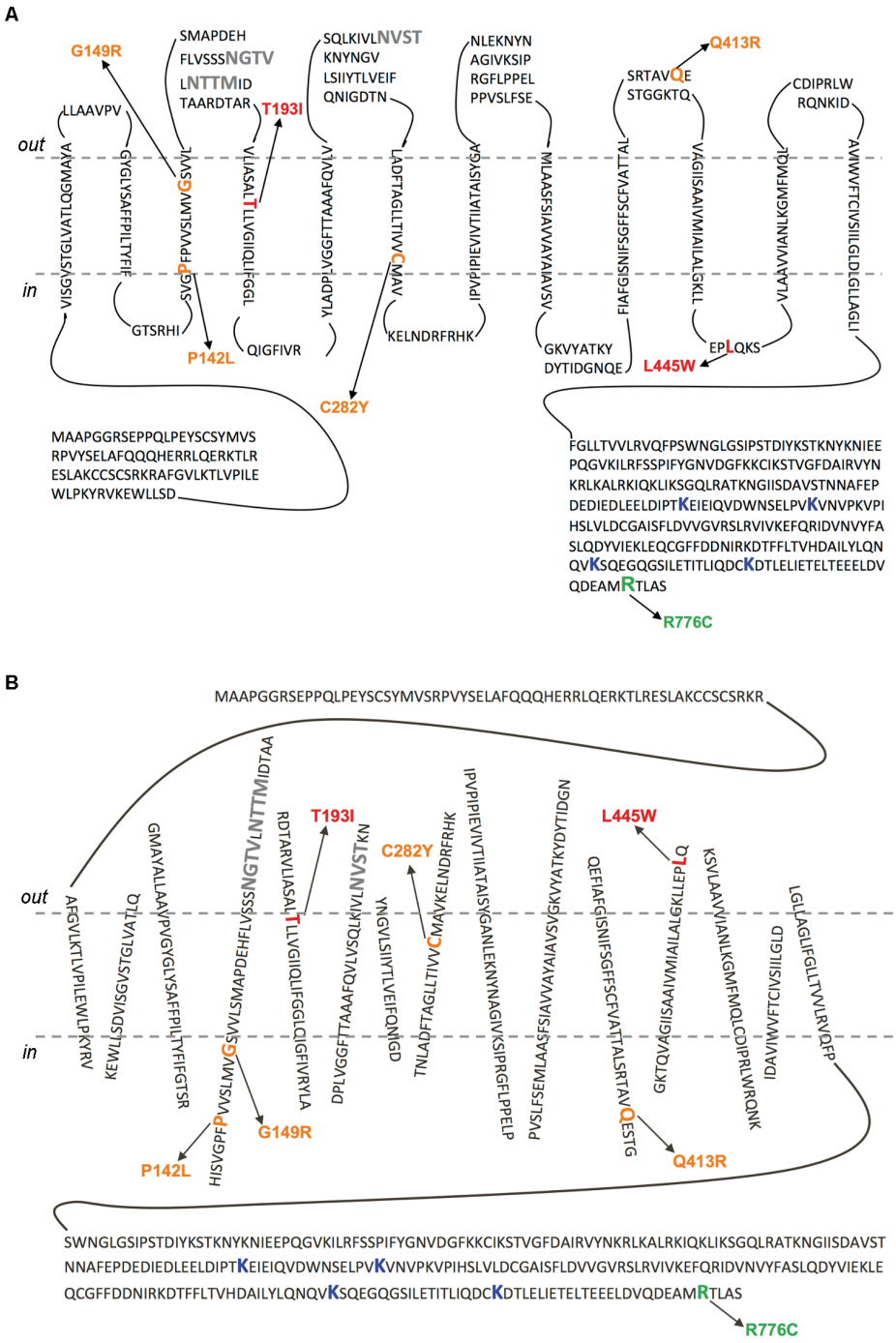

Supplementary Figure S1. Putative models of pendrin structure with positions of the amino acid substitutions of pendrin variants characterized in the present work and putative polyubiquitination and glycosylation sites. The models of pendrin structure (single letter amino acid code) are deduced from http://www.healthcare.uiowa.edu/labs/pendredandbor/domains.htm (A) and (10) (B). Amino acid substitutions marked in red and orange lead to loss and reduction of function, respectively. The amino acid substitution not affecting the function is represented in green. Lysine residues predicted to be polyubiquitination sites (http://www.ubpred.org/) are represented in blue. The predicted consensus sequences (Gene Runner, version 3.05) for N-glycosylation are represented by enlarged grey letters. The first two N-terminal glycosylation sites are experimentally confirmed for rat pendrin (11). Dotted lines indicate the plasma membrane. *In*, intracellular, *out*, extracellular. Panel B is reproduced with permission from Dossena S, *et al.* (2009) Functional characterization of wild-type and mutated pendrin (SLC26A4), the anion transporter involved in Pendred syndrome. *J Mol Endocrinol.* 43: 93–103.

Supplementary Table S1. Amplification primers for genomic DNA analysis of *GJB2, FOXI1* and *KCNJ10* (5′-3′).

GJB2 coding region			
Exon	Sense	Antisense	PCR product size (bp)
2	CTCCCTGTTCTGTCCTAGC	GACACGAAGATCAGCTGC	332
2	GCTACGATCACTACTTCCC	GGTTGCCTCATCCCTC	547
FOXI1 coding region			
Exon	Sense	Antisense	PCR product size (bp)
1	GTATAAGTGGGAGGCCGG	GCCAGCCCAGGTCG	422
1	CCAACGCCAGCCCC	GTAGCATCCCCCAGTCTTG	457
2	GTCTTCCTGCATCTGTCACC	GCTTTTCTCTCTGGCATGTC	716
KCNJ10 coding region			
Exon	Sense	Antisense	PCR product size (bp)
2	GTTAATTCCTCCCTCCCATG	CACATTGACCTGGTTGAGCC	794
2	GATCCGAGTTGCCAATATGC	GAGTGGAGGATGGGTGCTTC	663

The same primers were also used for sequencing.

Supplementary Table S2. Mutagenesis primers pairs and sequencing primers for plasmid DNA constructs (5′-3′).

SLC26A4 cDNA mutagenesis primers			
Amino acid substitution	Exon	Sense	Antisense
P142L	5	GTTGGACCTTTTC**T**AGTGGTGAGTTTAATGG	CCATTAAACTCACCACT**A**GAAAAGGTCCAAC
G149R	5	GAGTTTAATGGTG**A**GATCTGTTGTTCTGAGC	GCTCAGAACAACAGA**T**CTCACCATTAAACTC
T193I	5	GCCAGTGCCCTGA**T**TCTGCTGGTTGG	CCAACCAGCAGA**A**TCAGGGCACTGGC
C282Y	7	CACCATTGTCGTCT**A**TATGGCAGTTAAGG	CCTTAACTGCCATA**T**AGACGACAATGGTG
Q413R	10	CCCGCACGGCCGTCC**G**GGAGAGCACTGGAGG	CCTCCAGTGCTCTCC**C**GGACGGCCGTGCGGG
L445W	11	GCTTCTGGAACCCT**G**GCAGAAGTCGGTCTTGGC	GCCAAGACCGACTTCTGC**C**AGGGTTCCAGAAGC
R776C	21	CCAGGATGAGGCTATG**T**GTACACTTGCATCC	GGATGCAAGTGTAC**A**CATAGCCTCATCCTGG
SLC26A4 cDNA sequencing primers			
Name	Exon		
1R	5	TTCCATTGCTGCTGGATACG	
2R	9	GGAAAATGATGCAGCCAGC	
2F	5	TGGGATCTGTTGTTCTGAGC	
3R	15	TTGCCATAGAAAATAGGACTGG	
4F	14	GAAGCATCCCTAGCACAGATA	
981-98F	8	TGTTAAATCCATCCCAAG	

The nucleotide leading to the amino acid substitution is indicated in boldface. F, forward; R, reverse.

Supplementary Table S3. Evaluation of the transfection efficiency of constructs encoding pendrin variants.

	PDS-EYFP expressing cells	Cells not expressing PDS-EYFP	DsRed expressing (transfected) cells
WT PDS-EYFP IRES DsRed	7	0	7
T193I PDS-EYFP IRES DsRed	1 *,**	9	10
R776C PDS-EYFP IRES DsRed	13	0	13

Cells were transfected with pIRES2-DsRed-Express PDS-EYFP constructs encoding for wild-type (WT) pendrin or two representative variants with (T193I) or without (R776C) functional impairment. Cells expressing the indicated pendrin variants were identified based on the expression of EYFP. Transfected cells were identified based on the expression of the fluorescent protein DsRed. The significant reduction in the number of cells expressing T193I PDS-EYFP is not due to an impaired transfection, as those cells internalized the pIRES2-DsRed-Express PDS-EYFP construct and expressed the transfection marker DsRed. *,** $p < 0.001$ and $p < 0.0001$ vs wild type and R776C respectively, Fisher's exact test.

SUPPLEMENTARY REFERENCES

1. Dossena S, *et al.* (2011) Functional characterization of pendrin mutations found in the Israeli and Palestinian populations. *Cell Physiol. Biochem*. 28: 477-84.
2. Dossena S, *et al.* (2011) Identification of allelic variants of pendrin (SLC26A4) with loss and gain of function. *Cell Physiol. Biochem*. 28: 467-76.
3. Procino G, *et al.* (2013) Co-regulated pendrin and aquaporin 5 expression and trafficking in type-B intercalated cells under potassium depletion. *Cell Physiol. Biochem*. 32: 184-99.
4. Galietta LJ, Haggie PM, Verkman AS. (2001) Green fluorescent protein-based halide indicators with improved chloride and iodide affinities. *FEBS Lett*. 499: 220-4.
5. Dossena S, *et al.* (2006) Fast fluorometric method for measuring pendrin (SLC26A4) Cl^-/I^- transport activity. *Cell Physiol. Biochem*. 18: 67-74.
6. Yoshida A, *et al.* (2004) Mechanism of iodide/chloride exchange by pendrin. *Endocrinology*. 145: 4301-8.
7. Shcheynikov N, *et al.* (2008) The Slc26a4 transporter functions as an electroneutral $Cl^-/I^-/HCO_3^-$ exchanger: role of Slc26a4 and Slc26a6 in I^- and HCO_3^- secretion and in regulation of CFTR in the parotid duct. *J. Physiol*. 586: 3813-24.
8. Adler J, Parmryd I. (2010) Quantifying colocalization by correlation: the Pearson correlation coefficient is superior to the Mander's overlap coefficient. *Cytometry A*. 77: 733-42.
9. Morgan RA, *et al.* (1992) Retroviral vectors containing putative internal ribosome entry sites: development of a polycistronic gene transfer system and applications to human gene therapy. *Nucleic Acids Res*. 20: 1293-9.
10. Dossena S, *et al.* (2009) Functional characterization of wild-type and mutated pendrin (SLC26A4), the anion transporter involved in Pendred syndrome. *J. Mol. Endocrinol*. 43: 93-103.
11. Azroyan A, *et al.* (2011) Regulation of pendrin by pH: dependence on glycosylation. *Biochem. J*. 434: 61-72.